




**SPECIAL ISSUE PAPER****Recent advances in the study of Arctic submarine permafrost**

Michael Angelopoulos<sup>1,2</sup>  | Pier P. Overduin<sup>1</sup>  | Frederieke Miesner<sup>1</sup>  |  
Mikhail N. Grigoriev<sup>3,4</sup> | Alexander A. Vasiliev<sup>5,6</sup> 

<sup>1</sup>Alfred Wegener Institute Helmholtz Centre for Polar and Marine Research (AWI), Potsdam, Germany

<sup>2</sup>Institute of Geosciences, University of Potsdam, Potsdam, Germany

<sup>3</sup>Melnikov Permafrost Institute, Siberian Branch, Russian Academy of Sciences, Yakutsk, Russia

<sup>4</sup>Institute of Petroleum Geology and Geophysics, Siberian Branch, Russian Academy of Sciences, Novosibirsk, Russia

<sup>5</sup>Earth Cryosphere Institute of Tyumen Scientific Center, Siberian Branch, Russian Academy of Sciences, Russia

<sup>6</sup>Tyumen State University, Tyumen, Russia

**Correspondence**

Michael Angelopoulos, Alfred Wegener Institute Helmholtz Centre for Polar and Marine Research (AWI), Potsdam, Germany. Email: michael.angelopoulos@awi.de

**Funding information**

H2020 Societal Challenges, Grant/Award Number: 773421; Russian Foundation for Basic Research, Grant/Award Numbers: 18-05-60004, 18-05-70091

**Abstract**

Submarine permafrost is perennially cryotic earth material that lies offshore. Most submarine permafrost is relict terrestrial permafrost beneath the Arctic shelf seas, was inundated after the last glaciation, and has been warming and thawing ever since. As a reservoir and confining layer for gas hydrates, it has the potential to release greenhouse gasses and impact coastal infrastructure, but its distribution and rate of thaw are poorly constrained by observational data. Lengthening summers, reduced sea ice extent and increased solar heating will increase water temperatures and thaw rates. Observations of gas release from the East Siberian shelf and high methane concentrations in the water column and air above it have been attributed to flowpaths created in thawing permafrost. In this context, it is important to understand the distribution and state of submarine permafrost and how they are changing. We assemble recent and historical drilling data on regional submarine permafrost degradation rates and review recent studies that use modelling, geophysical mapping and geomorphology to characterize submarine permafrost. Implications for submarine permafrost thawing are discussed within the context of methane cycling in the Arctic Ocean and global climate change.

**KEYWORDS**

Arctic, offshore, submarine permafrost, subsea, thaw rates

**1 | INTRODUCTION**

Submarine permafrost has naturally received much less study than its terrestrial counterpart and remains largely unexplored under much of the Arctic shelf. We provide a review of recent contributions to the peer-reviewed literature that present new observational records, indirect evidence and advances in modelling of submarine permafrost. Our goal is to assess how these contributions are changing our understanding of the distribution of permafrost beneath the ocean and how permafrost changes over time.

Submarine permafrost is cryotic (<0°C) sediment and rock overlain by a marine water column. The terms offshore,<sup>1</sup> subsea,<sup>2</sup> and submarine<sup>3</sup> seem to be used in an equivalent manner in the literature, to describe sub-aquatic permafrost, beneath shelf seas and the ocean in general. In this paper, we err on the inclusive side by using the term 'submarine'. Submarine permafrost may or may not contain ice, depending on its temperature, salt content, sediment grain size and composition. This has led to the distinction between *ice-bonded*,<sup>4</sup> *ice-bearing*<sup>5</sup> and ice-free permafrost. Other terms used to describe permafrost in the Western literature include *ice-rich*,<sup>6</sup> *dry*,<sup>6</sup> *thaw-stable* and *thaw-unstable*<sup>7</sup> *thaw-sensitive* and *partially frozen*.<sup>8</sup> Most of these

This is an open access article under the terms of the Creative Commons Attribution License, which permits use, distribution and reproduction in any medium, provided the original work is properly cited.

© 2020 The Authors. Permafrost and Periglacial Processes published by John Wiley & Sons Ltd

terms are not quantitative, but refer, as in the case of *ice-bonded*, to a mechanical property of the earth material, or, as in the case of *ice-bearing*, to the presence of some ice. In the Russian literature, a distinction is made between *plastic* (deformable but containing crystalline ice) and ice-bonded sediment.

Most submarine permafrost occurs in the Arctic and is relict terrestrial permafrost<sup>9</sup> that was inundated when sea levels rose after the Last Glacial Maximum. Submarine permafrost is relevant to the global climate system by the stabilization of gas hydrates through cold temperatures,<sup>10</sup> the entrapment of gas by frozen sediment<sup>11</sup> and the storage of organic carbon.<sup>12,13</sup> There may be positive feedback between submarine permafrost thawing and climate warming by greenhouse gas release from or through the permafrost to the atmosphere.<sup>14</sup> Organic carbon thaw-out rates have been estimated near the Lena Delta on the East Siberian shelf,<sup>15</sup> for example. Submarine permafrost characterization is also critical to the design of offshore infrastructure, such as pipelines,<sup>16,17</sup> and for safe drilling practices for oil and gas exploration.<sup>18</sup>

It is estimated that 20 Gt C ( $2.7 \times 10^{13}$  kg CH<sub>4</sub>) may be sequestered in permafrost-associated gas hydrates, either as intra-permafrost and/or as sub-permafrost hydrates.<sup>19</sup> Free gas also exists and is released from permafrost sediments.<sup>20,21</sup> Permafrost thaw can destabilize gas hydrates<sup>3</sup> and may generate gas-migration pathways.<sup>22,23</sup> These findings are supported by recent lab experiments,<sup>24</sup> which demonstrate that salt migration can destabilize frozen hydrate-containing sediments. Observations of gas emission craters forming on land suggest that gas release can occur catastrophically.<sup>25</sup> Since the release of gas in these events seems to have been triggered by permafrost warming,<sup>26</sup> it is reasonable that the more advanced warming of permafrost below the seabed can cause similar events.

In the context of rapid warming and increasing human activity in the Arctic, we require a better understanding of submarine permafrost. In most settings, it has undergone rapid warming of about 10–15 °C due to marine transgression.<sup>27</sup> This is substantially more than the warming of about 2–4 °C currently observed in terrestrial permafrost.<sup>28</sup> Thus we expect permafrost warming and thaw to be further advanced in the submarine realm than in terrestrial environments.

The research considered in this paper was carried out in the past decade but builds on a substantial body of work that includes pioneering studies, many of which are not published in peer-reviewed journals. Research on subsea permafrost began in the 19th century, was taken up early in the 20th in the Soviet Union and flourished with the search for hydrocarbons on the Beaufort shelf beginning in the 1960s. Many valuable resources are contained in reports of the Outer Continental shelf Environmental Assessment Program (OSCEAP) of the Alaskan Bureau of Land Management and the U. S. National Ocean and Atmospheric Administration, the many Open File Reports of the Geological Survey of Canada<sup>29</sup> and monographs of the Russian Academy of Sciences. There are valuable resources, citing relevant research on the Arctic shelves in the eastern and western hemispheres.<sup>30,31</sup> Research activity has increased during the 2010s, perhaps partly as a result of the surprising rate of sea ice retreat, which

promises to change conditions for submarine permafrost and to improve access to shelf regions.

## 2 | RECENT WORK ON SUBMARINE PERMAFROST

### 2.1 | Observations on presence or absence of permafrost

#### 2.1.1 | Geomorphology

Seabed features that may be associated with permafrost include pockmarks, pingo-like features<sup>10,32</sup> and what may be thermokarst basins infilled with marine sediment.<sup>33,34</sup> Morphological similarity suggests that the latter are submarine expressions of the same processes that have led to *cryovolcanism*, a term used to describe the appearance of craters due to the expulsion of gas from warming permafrost.<sup>35</sup> These features lie partially in the gas hydrate stability zone and were capped by Quaternary marine sediments at differing times depending on bathymetry and neotectonics.<sup>34</sup> Sub-aquatic pingo-like features have also been observed by ground-penetrating radar surveys along deformed bed-ice contacts in Lake Vida, Antarctica.<sup>36</sup> Polygonal features on the sea floor<sup>23</sup> may reflect ongoing thaw of deep ice wedges (i.e. down to 15 m below sea level) after submergence. In bedfast ice zones, talik initiation may be delayed due to atmosphere-seabed coupling in winter.<sup>37</sup> In addition, submerged sand bars may lead to localized and temporary submarine permafrost formation (Figure 1b), as well as cold hypersaline waters towards the coast. Even if submarine permafrost is degrading, this process may create a sub-aquatic layer of seasonally frozen ground beneath floating ice.<sup>38</sup>

Concentrated brines at low temperatures that form in shallow water zones during sea ice freezing or in transgressive sediment strata beneath the shelf may prevent ice formation by lowering the freezing point of the porewater, resulting in a cryopeg (Figure 1g). The exclusion of dissolved solids during freezing creates hypersaline cryopegs, which may be widespread along Arctic coasts containing refrozen marine sediments.<sup>39</sup> The brines created by freezing may lead to thermodynamic disequilibrium and the precipitation of minerals,<sup>40</sup> which is also characteristic of hypersaline springs in the Canadian High Arctic.<sup>41</sup> Cryopegs, with low ice content, may be sites of free gas accumulation and speed the rate of thaw relative to ice-saturated permafrost.

#### 2.1.2 | Geophysical methods and remote sensing

Various techniques have been used to observe the distribution of submarine permafrost, and recent innovations are leading to improved spatial coverage of mapping efforts. The combination of seismic methods with borehole geophysical records has led to the only maps

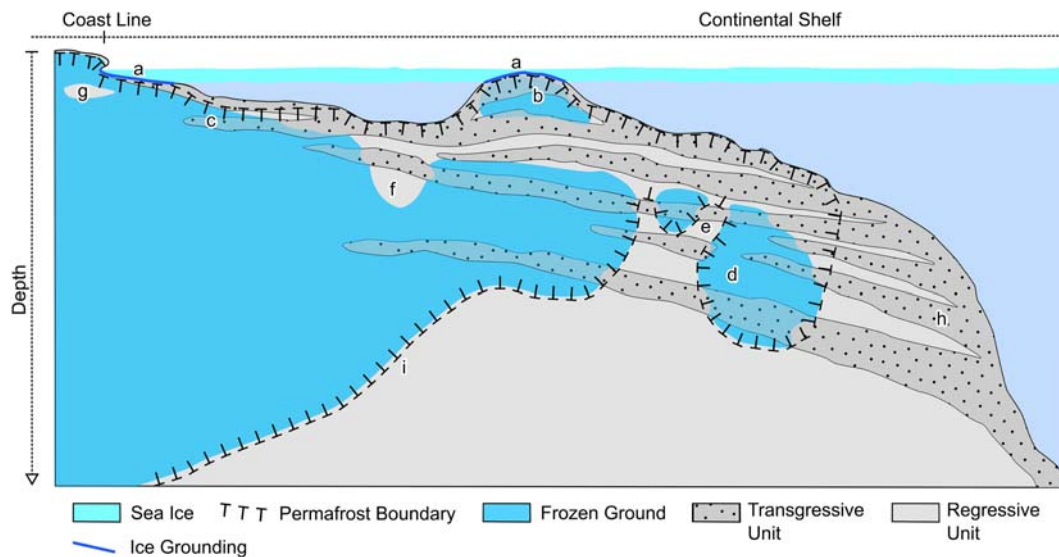


**FIGURE 1** Schematic of offshore permafrost. Shown are a) ice grounding at the coast and in shallows, b) aggrading and c) degrading permafrost zones, d) ice bearing permafrost (IBP), e) an open talik, f) a talik, g) a cryopeg, h) onlapping transgressive sediment strata, and i) the lower permafrost boundary

of permafrost extent and depth beneath the Arctic Ocean that are based on direct observations. Core material was not recovered from most boreholes and, of those which were cored, few underwent scientific analysis. A few deeper cores were analysed and showed alternating regressive and transgressive sediment cycles (Figure 1h) of thick clastics and thin marine muds, respectively.<sup>42</sup> Multi-reflection seismic data have been used to map the minimum extent of submarine permafrost on the Alaskan Beaufort shelf,<sup>43</sup> which has been compared to borehole records<sup>44</sup> and refraction seismic data collected in earlier studies.<sup>45</sup> Borehole records were also interpreted for the Canadian Beaufort shelf.<sup>46</sup> Furthermore, the extent of submarine permafrost has been reported for the Kara Sea based on seismic observations.<sup>47,48</sup> Multichannel reflection seismic techniques have also been applied to map the base of the gas hydrate stability zone beneath submarine permafrost in the Canadian Beaufort Sea.<sup>18</sup> Although reflection and refraction seismology have been the most common tool to map subsea permafrost, passive approaches are promising new techniques that use ambient noise to identify sharp wave velocity contrasts, which may be interpreted as boundaries between unfrozen sediment and ice-bearing permafrost (IBP).<sup>49</sup>

Electrical resistivity surveying is also effective at mapping the top of shallow ice-bearing submarine permafrost, because the resistivity of frozen material is higher than that of unfrozen material for a specific sediment type and salinity. In electrical resistivity surveying, the top of IBP is inferred from bulk sediment resistivity values inverted from observed apparent resistivities. Recent studies have applied this strategy offshore of the Bykovsky Peninsula<sup>50</sup> and Muostakh Island in Siberia,<sup>51</sup> as well as off the coast of Barrow, Alaska.<sup>52</sup> The electrical resistivity of ice-bearing sediment is very sensitive to salinity, approaching values lower than 10  $\Omega\text{m}$ .<sup>52</sup> The technique is also effective at delineating seasonal coastal permafrost changes as a means to explain coastal erosion rates,<sup>53</sup> as well as detecting deep coastal

permafrost degradation from seawater intrusion.<sup>54</sup> Electrical resistivity surveying is not limited to saline waters and can be used to map talik geometry beneath thermokarst lakes<sup>55</sup> and in fresh or brackish water offshore. Ground-penetrating radar has been shown to be effective at mapping sub-aquatic frozen sediment beneath non-saline bedfast ice zones in the Mackenzie Delta, Canada.<sup>56</sup> Transient electromagnetics (TEM) have been used to map a deep talik beneath a thermokarst lake on the Alaskan coastal plain<sup>57</sup> and can be used offshore. For example, TEM was used to map the vertical extent of permafrost in the central Laptev Sea.<sup>58</sup>

The methods mentioned earlier provide a means of measuring the top of the IBP (Figure 1d) in areas of thick permafrost. Geophysical methods capable of detecting both the upper and lower (Figure 1i) phase change boundaries of thick permafrost permit detection of total thaw rates and of ice-free pathways perforating the permafrost. Controlled source electromagnetics (CSEM) have been used in deeper marine environments for delineation of hydrates. Recent application of a shallow water version of the method on the Alaskan Beaufort shelf has resulted in inversion of resistivity for the sediment column containing permafrost.<sup>59,60</sup>

Advances in satellite remote sensing have changed our understanding of the effect of permafrost on landscape and vegetation over the past decades and at larger spatial scale than possible with land-based studies, but submarine permafrost is largely invisible to satellite remote sensing methods. The application of radar backscatter and coherence time series is useful for bedfast ice detection in thermokarst lakes<sup>61</sup> and the marine environment.<sup>62</sup> Satellite remote sensing is not currently used to observe warming or thawing of submarine permafrost, but it can be useful to detect methane emissions from the Arctic seas.<sup>63</sup> In addition to filling in an otherwise-blank map of permafrost distribution, these recent results provide validation data for models of submarine permafrost.

## 2.2 | Glaciation

In general, deep permafrost develops in regions that were exposed during the persistently cold climate of glacial periods, although permafrost may form below ice caps with cryotic basal ice temperature regimes. Modern submarine permafrost distribution was affected by glaciation on the current shelf,<sup>27</sup> with thick permafrost below unglaciated shelves (Figure 2). Recent publications are challenging our understanding of past Arctic ice extents, however, with implications for permafrost distribution.<sup>64-66</sup> There is bathymetric and seismic evidence of repeated grounding of ice sheets and shelves on the East Siberian shelf in previous glacial cycles,<sup>67</sup> presumably centred around the New Siberian Islands.<sup>68</sup> Furthermore, our understanding of the probable timing of ice sheet advances on the Canadian Beaufort shelf is developing.<sup>69,70</sup> Ice sheet development may have been initiated in Alaska during interglacials and have covered the North Slope and

shelf.<sup>71</sup> Some of these studies provide evidence for large glacial ice masses during the penultimate glacial period, which may have had little direct effect on current subsurface temperature distribution, but an indirect effect through glacial isostatic adjustment<sup>72</sup> and sediment dynamics on the shelf.

## 2.3 | Coastal processes

Coastal erosion leads to retreat of the shoreline and the creation of submarine permafrost below the region of land loss. For example, about 10 km<sup>2</sup> of land per year is inundated along the East Siberian coast,<sup>76</sup> a process that has increased in rate by a factor of 1.5–2 since about 2004.<sup>77</sup> At Drew Point, Alaska, the mean erosion rate from 2007 to 2016 was 2.5 times greater than the historical average.<sup>78</sup> Along the Yukon Coastal Plain, coastal erosion rates have been

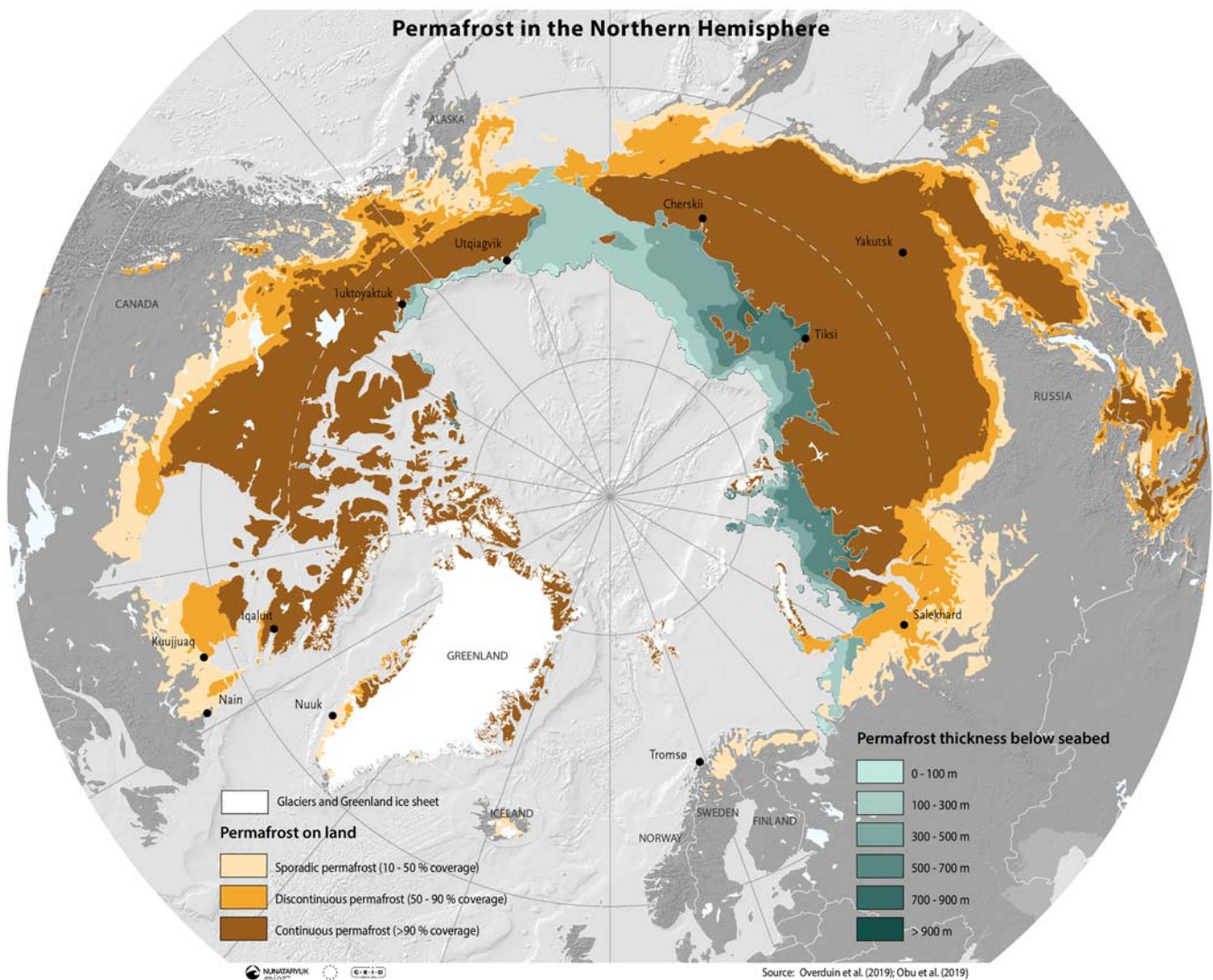


**FIGURE 2** The distribution of cryotic (<0 °C) sediment below the Arctic shelf based on numerical modelling<sup>27</sup> is shown here together with terrestrial permafrost probability.<sup>73</sup> The area of subsea permafrost shown is  $2.5 \times 10^6$  km<sup>2</sup> of the Arctic shelf. The data sets are available online,<sup>74,75</sup> and the map is available from GRID-Arendal (<https://www.grida.no/resources/13519>)

increasing since the 1990s.<sup>79</sup> Once inundated, seawater may intrude and salt diffuse into the sediment, affecting permafrost below the seabed or laterally close to the coast. Seawater can intrude into coastal permafrost<sup>54</sup> and may facilitate thermokarst development in retrogressive thaw slumps. In the case of lagoons, the degradation of a refrozen thermokarst lake talik may occur following seawater intrusion.<sup>80</sup> Thus, lagoons may pre-condition the sediment with saline porewater during the transition of permafrost from terrestrial to submarine. The seasonal isolation of shallows through sea ice grounding can lead to brine entrapment.<sup>81</sup> Lagoons and other shallow depressions near the coast<sup>76</sup> may be more saline than the nearshore zone. In the eastern Alaskan Beaufort Sea, lagoons form more than 70% of the coastline and experience large annual changes in temperature and salinity, including the development of hypersalinity.<sup>82</sup> Thus, temperature and salt concentrations at the seabed may vary considerably spatially and temporally, affecting the submarine permafrost degradation rate.

Through heat advection, groundwater flow can act to speed permafrost thaw and shrink the hydrate stability zone<sup>3</sup> and facilitate methane gas diffusion to the surface.<sup>23</sup> However, over multiple glacial cycles, submarine groundwater discharge may freshen marine sediment porewater and increase the freezing point to preserve submarine permafrost and increase gas hydrate stability.<sup>3</sup> Methane in Arctic waters may also originate from the land and be transported through submarine groundwater discharge conduits.<sup>83</sup> Recent observations also suggest that sub-permafrost groundwater flow leads to freshening of the Arctic seas off the Siberian shelf.<sup>84</sup> In the Canadian Beaufort Sea, freshwater seepage into shelf, shelf-edge and slope sediments was observed and attributed to top-down infiltration of mixed sea and river water, subsea permafrost degradation and submarine groundwater discharge.<sup>85</sup> The freshening of coastal bottom waters is affected by riverine runoff. In northeastern Siberia, discharge from the Lena River has increased over the last several decades, mostly during the winter.<sup>86</sup> Factors affecting discharge and sediment load include neotectonic processes, thermokarst, as well as hydraulic connections between the river and the underlying talik.<sup>87</sup> Offshore, water flow within the thawed layer may also be due to convective processes: recent fieldwork in the Kara Sea revealed upward water advection in subsurface sediments with convection from thawing submarine permafrost as a possible explanation.<sup>88</sup> Such processes act to accelerate submarine permafrost thawing and could contribute to the destabilization of gas hydrates.

## 2.4 | Global climate forcing and permafrost thaw

Inundation of the East Siberian shelf invokes a change from ground surface temperatures of -15 to -10 °C to sea bottom temperatures, which are typically between -2 to -0.5 °C in areas unaffected by freshwater from rivers.<sup>89</sup> The seabed is separated from atmospheric forcing by sea ice and the water column. The large thermal inertia associated with the latent heat of phase change of water, and the nearness of seabed temperatures to the phase change temperature,

ensure that submarine permafrost reacts slowly to imposed changes. The hydrodynamic shallow Arctic coast and the presence of moving ice for much of the year have made it difficult to collect time series of sediment temperature.

The release of greenhouse gas is potentially more important to the global climate than the heat energy component associated with permafrost thaw. An abrupt and large release of greenhouse gases may significantly affect global climate, especially if released as methane rather than CO<sub>2</sub>, but the origin, stocks, spatial distribution and stability of methane beneath the Arctic shelf remain controversial. Estimates for the amount of gas hydrate associated with permafrost in the Arctic are around 1 % of global gas hydrates or 20 Gt.<sup>19</sup> This does not include offshore organic carbon tied up in permafrost that could be metabolized to methane or carbon dioxide after thawing. Within submarine organic carbon pools, methane probably occupies a higher proportion of carbon products.<sup>14</sup> The challenge from a permafrost perspective is one of attribution: are observations of gas emission on the Arctic shelf related to permafrost thaw, given that they are also common in many non-permafrost regions? The most significant physical barrier is IBP with low gas diffusivity,<sup>11</sup> which entraps gas beneath and within IBP. This gas may be released through permafrost thaw, for example through the formation of open taliks<sup>23</sup> or the destabilization of gas hydrates within IBP.

The stability of hydrates depends on coupled temperature-pressure conditions and can be as shallow as 20 m below the seabed. A summary of the history of Arctic gas hydrates, as well as the mechanisms for their formation, has been provided.<sup>22</sup> Although important methane fluxes attributed to submarine permafrost thaw have been reported in the East Siberian shelf, any released gas must migrate past numerous physical and chemical sinks before it can reach the atmosphere.<sup>10</sup> For example, methane may be microbially oxidized in the unfrozen sediment column above ice-rich permafrost, as observed in the Laptev Sea.<sup>51</sup> The proliferation of bacteria in warmed submarine permafrost and the microbial communities responsible for anaerobic oxidation of methane have been described,<sup>90,91</sup> and similar processes have been investigated for thermokarst lakes.<sup>92</sup> In the Beaufort Sea, most methane in surface waters is not from ancient sources,<sup>93</sup> suggesting that the release of ancient carbon methane into bottom waters is mitigated by effective oxidation and dispersion in the water column. Methane that reaches the water column may be absorbed into sea ice and transported into the deep ocean through ice drift.<sup>94</sup> Given sea ice's role as a methane sink, decreasing sea ice coverage in the Arctic could also increase methane fluxes to the atmosphere. Clearly, further research regarding methane pathways from shelf sediments into sea ice is needed, as well as how methane stocks in the sea ice and water column change seasonally.

A link has been drawn by numerous authors between ebullition and high methane concentrations in shallow submarine sediment, seawater and the atmosphere on the one hand and submarine permafrost thaw on the other.<sup>21,23,32,95,96</sup> This connection may exist where permafrost is present and thawing in the presence of observed gas emissions, but this simultaneity does not mandate a permafrost or gas hydrate source. For example, at locations where permafrost has

persisted for multiple glacial cycles, sub-permafrost gas may have migrated upwards and become incorporated into the permafrost during subsequent glacial periods (intra-permafrost).<sup>97</sup> Gas within and below the permafrost may have undergone numerous transitions between the hydrate stability zone and instability. Isotopic signatures of atmospheric methane do not indicate an Arctic seabed source for observed increases,<sup>98</sup> and there is now evidence that previous estimates of methane release rates were probably too high.<sup>99</sup> Modelling efforts suggest that marine hydrates dissociate too slowly or in insufficient amounts to create a strong positive feedback effect.<sup>100</sup> More observational data from the large East Siberian shelf region, in particular, and from seasons other than late summer and early autumn, will improve our estimates of greenhouse gas exchange between the seabed, water column, sea ice and atmosphere.

## 2.5 | Rates of degradation

There are few observational data on the rate of submarine permafrost thaw. The apparently slow rates of permafrost thaw beneath the seabed mandate long time periods for repeat observations. Uncertainties in the position of historical boreholes make it difficult to perform repeat measurements. The lack of regional sea level curves for the Arctic shelf and the dynamic sediment regime in shallow waters make it difficult to estimate inundation periods for locations where the depth to ice-bonded permafrost is known.

In Figure 3, estimates of the ice-bonded permafrost table depth from borehole measurements are plotted against estimated inundation times. Borehole data are available in the cited studies. Permafrost depths for a given inundation time vary considerably across the circum-Arctic. For these shallow shelf sites, variability is driven mostly by regional seawater and salinity regimes. For inundation times less

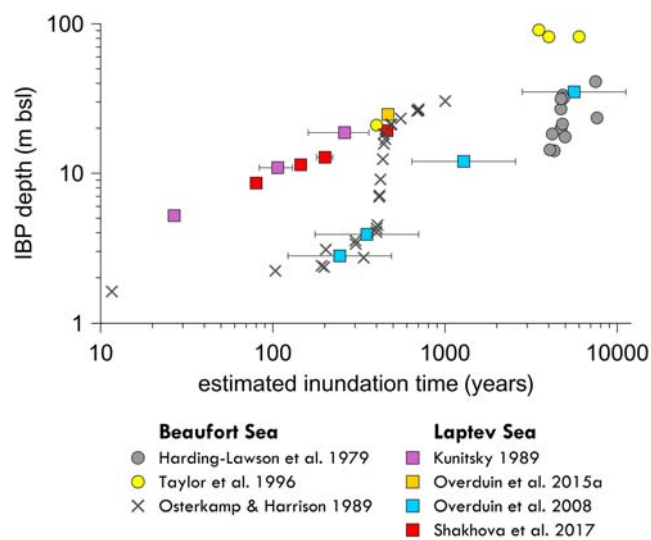


**FIGURE 3** Borehole determinations of submarine ice-bonded permafrost depths plotted against estimated periods of inundation from studies in the Laptev and Beaufort Seas

than 400 years, the deepest depths to ice-bonded permafrost were observed offshore of Muostakh Island in the Laptev Sea. This area is affected by the warm freshwater discharge of the Lena River and has a mean annual bottom water temperature of  $0.5^{\circ}\text{C}$ <sup>51</sup> close to the island's north tip. The ice-bonded permafrost depth increased from 16.8 to 19.3 m below sea level (BSL) from 1982 to 2014 at the borehole farthest offshore of Muostakh Island.<sup>23</sup> While the high degradation rate may be partially attributed to warming shelf waters, there is a lag between ocean warming and accelerated deepening of the upper boundary of frozen sediments.<sup>101,102</sup> In any case, the ice-bonded permafrost depths are similar to other data from the region<sup>103,104</sup> when considering the total time since inundation. Interestingly, the ice-bonded permafrost depths offshore of Tiksi Bay are at least four times greater than those in the western Laptev Sea, where the ice-bonded permafrost depths were only 4 m bsl 400 years after submergence.<sup>105</sup> We attribute the shallower depths to colder, negative mean annual bottom water temperatures. Modelling shows that the degradation of submarine permafrost from salt diffusion in an area with a mean annual bottom water temperature of  $-0.7^{\circ}\text{C}$  can be less than half the rate of degradation from an advancing thawing front in waters with a mean annual bottom water temperature of  $0.5^{\circ}\text{C}$ .<sup>50</sup> The latter assumes diffusion as the dominant mechanism for salt transport, which is increasingly stable in fine sediment with low hydraulic conductivity.

On the Alaskan Beaufort shelf, the sediment is typically more coarse-grained than the silty sands at the sites described earlier. This may facilitate interstitial water movement and salt transport in the thawed layer, increasing the degradation rate.<sup>106</sup> For example, offshore of Prudhoe Bay where the mean bottom water temperature is negative, the ice-bonded permafrost depths<sup>2</sup> are similar to those observed offshore of Muostakh Island and in Tiksi Bay for similar inundation times.

On the comparatively steep Beaufort shelf, the ice-bonded permafrost depths observed offshore of the Mackenzie Delta are at least two times greater than those of the Alaskan Beaufort Sea<sup>107</sup> for inundation times greater than 4000 years. This is largely because of the Mackenzie River discharge, which contributes to mean annual bottom water temperatures above  $0^{\circ}\text{C}$  nearshore after inundation.<sup>1</sup> The effect may be enhanced by more thermally conductive and less ice-rich sediment. In the Canadian Beaufort Sea, the ice-bonded permafrost depth is not always positively correlated with inundation time estimated from geothermal modelling.<sup>1</sup> For example, the depth to ice-bonded permafrost is 91 m bsl (3 m water depth) at 3500 years of inundation compared to 82 m bsl (32 m water depth) for 6000 years of inundation. Both the borehole locations mentioned earlier are characterized by similar post-transgressive sediment thicknesses. Holocene thermokarst lakes with taliks may have existed prior to the marine transgression and may be partly responsible for the deep thaw and apparent high rates of coastal retreat close to Richards Island.<sup>1</sup> Recent numerical modelling shows that the warm outflow plume of the Mackenzie River results in an ice-bonded permafrost table depth of 100 m below the sea floor (bsf) nearshore compared to 50 m bsl beyond the 20 m isobath.<sup>108</sup> The presence of bedfast ice and seasonal

freezing of the seabed in shallow floating ice zones also has a major impact on submarine permafrost depths. The top of ice-bonded permafrost may not decouple from the seasonally frozen layer until 400m offshore as shown from boreholes near Prudhoe Bay, Alaska.<sup>2</sup> Assuming a coastal erosion rate of 1 m/a, this corresponds to an inundation time of 400 years. Therefore, talik development may be delayed or slowed down in areas where bedfast ice and cold saline water below sea ice are a factor. This is further demonstrated by modelling of submarine permafrost<sup>50</sup> and shallow thermokarst lakes.<sup>109</sup> Although the sites compared here have diverse geological histories and boundary conditions for submarine permafrost, their IBP depths imply mean annual degradation rates of metres to less than centimetres per year, slowing with increasing duration of inundation.

## 2.6 | Advances in modelling

Study of the seabed and deeper sediment is difficult in a shallow-water environment that hinders access for larger ships and where sea ice can threaten any seabed or floating infrastructure. As a result, a number of studies use numerical modelling of submarine permafrost to study its distribution and the processes that affect it. The timing of exposure of the continental shelf (by marine regressions) and the duration of inundation with seawater (by transgressions) determine the thermal state of the sediment.<sup>27,110</sup> In numerical simulations, newly submerged permafrost reaches an almost isothermal temperature profile over a 1 km depth within a few millennia after inundation.<sup>27</sup> New models that account for advection show that submarine groundwater discharge may be an important factor determining submarine IBP extent and gas hydrate stability in the Beaufort Sea over multiple glacial cycles.<sup>3</sup> In addition, gas hydrate stability models demonstrate that methane gas venting to the water column may be facilitated by deep taliks below paleo-river channels.<sup>96</sup> Advances in modelling also include the coupling of diffusive heat and salt flow in the sediment for the top-down degradation of IBP,<sup>50,101</sup> as well as for sea ice dynamics and the seasonal freezing of the seabed.<sup>111</sup> Salt diffusion minimizes seasonal freezing of the seabed in Tiksi Bay,<sup>111</sup> which is characterized by positive mean annual bottom water temperatures.<sup>51</sup> The mitigation of seasonal freezing from salt can lead to faster submarine permafrost degradation rates in warm coastal waters affected by terrestrial river runoff.<sup>50</sup>

In most of the Siberian Arctic shelf, however, cold and saline bottom water with mean annual negative temperatures acts to preserve submarine permafrost (Figure 1a). In bedfast ice zones, conditions may be sufficiently cold to preserve ice in the permafrost. Despite submarine permafrost preservation, a cryotic talik (Figure 1f) still develops when the mean annual negative bottom water temperature is higher than the mean annual freezing point of the water. Models show that the development of open taliks (Figure 1e) occurs in areas of high geothermal heat flow after long inundation periods,<sup>112</sup> and may be facilitated by inundated thermokarst lake taliks<sup>113</sup> and sediments already saline when submerged.<sup>114,115</sup>

Sediment will also respond differently to heat flow depending on its properties. For example, increased porosity and thus ice content in saturated sediment will reduce thaw rates, particularly for ice-rich ground close to the surface. Deeper in the subsurface where sediments are compacted, higher thermal conductivity results in more rapid thawing of the submarine permafrost's lower boundary. The sediment type not only controls the freezing characteristic curve but also the interaction with salt. In coarse-grained sediments, interstitial water movement can speed salt transport. First and foremost, this may result in more vertical salinity profiles in the talik, thus enhancing salt diffusion at the phase-change boundary (IBP table). Second, in the case of submerged thermokarst lake taliks, this may prevent refreezing if the freezing point of the sediment porewater is sufficiently depressed before arrival of the freezing front. As thawing progresses, the salt concentration gradient over depth flattens and diffusion slows down. In empirically based models, it has been shown that thawing due to salt diffusion is negligible below about 30 m beneath the seabed.<sup>102,116</sup>

While warming ocean waters may increase the degradation rate of newly submerged permafrost, coupled heat and salt simulations suggest that recent warming of the Siberian Arctic shelf over the past few decades,<sup>101</sup> presumably as a result of changing climate, sea ice cover and ocean circulation,<sup>117</sup> is unlikely to affect deep hydrate-bearing permafrost until the next millennium. Recent modelling suggests that subtle changes in bottom water temperature and geothermal heat flow since the onset of the latest marine transgression on the West Yamal Shelf determine the presence or absence of submarine permafrost<sup>118</sup> over long inundation periods. At a larger scale, submarine permafrost is mapped consistently for the circumarctic region using numerical modelling of the sediment temperature evolution over the last 50 ka forced by distributed geothermal heat flux, transient air temperature, ice cap dynamics and sea level history.<sup>27</sup> Through regional validation from seismically delineated frozen sediment, the modelled submarine permafrost underlies  $2.5 \times 10^6$  km<sup>2</sup> of the Arctic shelf (Figure 2) and over 97 % of it is thawing at the permafrost's lower boundary.

## 3 | CONCLUSION

New observations are needed to improve our understanding of the distribution and dynamics of submarine permafrost in the Arctic, either via direct measurements through sediment coring or via indirect assessments through geophysical methods or the collection of permafrost-relevant data. Recent advances in shallow controlled-source electromagnetics and passive seismic methods promise to bring new insights into the distribution and degradation of submarine permafrost. Despite limited field data, large-scale modelling has helped drive our understanding of submarine permafrost's spatial extent and thickness. The results are promising, given that there is good agreement between modelled outputs and field observations. Recent research on coupled heat and salt diffusion

models that include seasonal sea ice and seabed freeze/thaw processes demonstrates that coastal settings can be close to equilibrium, with either degrading or aggrading permafrost depending on boundary conditions soon after inundation. This is particularly important for coastal infrastructure design and the potential release of greenhouse gas. Future research should aim to incorporate interstitial water flows as part of heat and salt transport models in areas where diffusive regimes are thought or observed to be unstable. This would be valuable for areas affected by thermokarst lake taliks prior to submergence, as the rapid transport of salt into the sediment could prevent taliks from refreezing and favour development of open taliks, which are potential conduits for gas transport. Studies of the distribution of gas sources and provenance are needed to provide a basis for an Arctic-wide assessment of fluxes associated with the Arctic shelf and its permafrost. Methods to distinguish deep hydrate sources from shallower intra-permafrost and marine sediment sources will be a necessary part of these studies. Our evolving understanding of past Arctic glaciations in terms of geographic extent, thickness and timing will change our understanding of the distribution and state of permafrost and the hydrate stability zone over glacial-interglacial time scales. The International Continental and Oceanic Drilling programmes' commitment to joint missions creates an avenue for investigations of the transition from deep, cold terrestrial to warm, offshore permafrost, along with the suite of paleo-environmental, deep microbiological and geological questions that could be addressed on the understudied Arctic shelf.

## ACKNOWLEDGEMENTS

This publication is part of the Nunataryuk project. The project has received funding under the European Union's Horizon 2020 Research and Innovation Programme under grant agreement no. 773421. Submarine permafrost studies in the Kara and Laptev seas were supported by Russian Foundation for Basic Research (RFBR/RFFI) grants #18-05-60004 and #18-05-70091, respectively. The International Permafrost Association (IPA), the Climate and Cryosphere core project (CliC) of the World Climate Research Programme (WCRP) and the Association for Polar Early Career Scientists (APECS) supported research coordination that led to this study. Data that support the findings in this paper are available from the references cited in Figure 2 and Figure 3, for which DOIs are listed in the reference lists. Prof. Dr. Hans-Wolfgang Hubberten contributed to this effort by integrating the international community at an early stage and through his contributions on submarine permafrost. We also thank Dr. Christopher Burn, Dr. Mauro Guglielmin, Dr. Benjamin Jones and an anonymous reviewer for their helpful comments on the manuscript.

## ORCID

Michael Angelopoulos  <https://orcid.org/0000-0003-2574-5108>

Pier P. Overduin  <https://orcid.org/0000-0001-9849-4712>

Frederieke Miesner  <https://orcid.org/0000-0002-2849-0406>

Alexander A. Vasiliev  <https://orcid.org/0000-0001-5483-8456>

## REFERENCES

1. Taylor AE, Dallimore SR, Outcalt S. Late Quaternary history of the Mackenzie-Beaufort region, Arctic Canada, from modelling of permafrost temperatures. 1. The onshore-offshore transition. *Canad J Earth Sci.* 1996;33(1):52-61. <https://doi.org/10.1139/e96-006>
2. Osterkamp TE, Baker GC, Harrison WD, Matava T. Characteristics of the active layer and shallow subsea permafrost. *J Geophys Res Oceans.* 1989;94(C11):16227-16236. <https://doi.org/10.1029/JC094iC11p16227>
3. Frederick JM, Buffett BA. Effects of submarine groundwater discharge on the present-day extent of relict submarine permafrost and gas hydrate stability on the Beaufort Sea continental shelf. *J Geophys Res Earth Surface.* 2015;120(3):417-432. <https://doi.org/10.1002/2014JF003349>
4. Hunter JA, Judge AS, MacAulay HA, Good RL, Gagne RM, Burns RA. The occurrence of permafrost and frozen subsea bottom materials in the southern beaufort sea. Beaufort sea project. Technical Report 22, Victoria, BC, Canada, Department of the Environment, Canada; 1976.
5. Barnes PW, Hopkins DM. Earth sciences. *Environmental assessment of the Alaskan Continental Shelf, interim synthesis report: Beaufort/Chukchi, august, 1978*, Outer Continental Shelf Environmental Assessment Program. Washington, DC, USA: Environmental Research Laboratory, National Oceanic and Atmospheric Administration, Department of Commerce; 1978:101-131.
6. Brown RJE, Kupsch WO. Permafrost terminology (Technical Memorandum III), Ottawa, Ontario, Canada, National Research Council of Canada; 1974.
7. Linell KA, Kaplar CW. Description and classification of frozen soils. In: Permafrost, Proceedings of An International Conference National Academy of Sciences; 1966; Washington, DC, U.S.A.:481-487.
8. van Everdingen RO. Geocryological terminology. *Canad J Earth Sci.* 1976;13:862-867.
9. Kitover DC, van Balen RT, Vandenberghe J, Roche DM, Renssen H. LGM permafrost thickness and extent in the Northern Hemisphere derived from the Earth System Model iloveclim. *Permafr Periglac Process.* 2015;27(1):31-42. <https://doi.org/10.1002/ppp.1861>
10. Ruppel CD, Kessler JD. The interaction of climate change and methane hydrates. *Rev Geophys.* 2017;55(1):126-168. <https://doi.org/10.1002/2016RG000534>
11. Chuvilin EM, Grebenkin SI, Sacleux M. Influence of moisture content on permeability of the rocks in the frozen and thawed condition. *Earth Cryosphere.* 2016;20(3):66-72. [http://izdatgeo.ru/pdf/earth\\_cryo/2016-3/66\\_eng.pdf](http://izdatgeo.ru/pdf/earth_cryo/2016-3/66_eng.pdf)
12. Vonk JE, Sánchez-García L, Van Dongen B, et al. Activation of old carbon by erosion of coastal and subsea permafrost in Arctic Siberia. *Nature.* 2012;489:137-140. <https://doi.org/10.1038/nature11392>
13. McGuire A, Anderson LG, Christensen TR, et al. Sensitivity of the carbon cycle in the Arctic to climate change. *Ecol Monog.* 2009;79(4):523-555. <https://doi.org/10.1890/08-2025.1>
14. Schuur E, McGuire A, Schädel C, et al. Climate change and the permafrost carbon feedback. *Nature.* 2015;2015:171-179.
15. Wild B, Shakhova N, Dudarev O, et al. Organic matter across subsea permafrost thaw horizons on the East Siberian Arctic Shelf. *Cryosphere Discuss.* 2018;2018:1-26. <https://doi.org/10.5194/tc-2018-229>
16. Bashaw E, Hebel G, Phillips W, Kane G. Geologic and subsea permafrost characterization for buried pipeline design and construction in the Alaskan Beaufort Sea. *Arctic Technology Conference.* St. John's, Newfoundland and Labrador, Canada: Offshore Technology Conference; 2016:15. <https://doi.org/10.4043/27450-MS>
17. Paulin M, Caines J. The evolution of design tools for Arctic subsea pipelines. *Arctic Technology Conference.* St. John's, Newfoundland and Labrador, Canada: Offshore Technology Conference; 2016:11. <https://doi.org/10.4043/27374-MS>



18. Riedel M, Brent T, Taylor G, et al. Evidence for gas hydrate occurrences in the Canadian Arctic Beaufort Sea within permafrost-associated shelf and deep-water marine environments. *Marine Petroleum Geology*. 2017;81:66-78. <https://doi.org/10.1016/j.marpetgeo.2016.12.027>
19. Ruppel CD. Permafrost-associated gas hydrate: Is it really approximately 1% of the global system? *Journal of Chemical and Engineering Data*. 2015;60:429-436. <https://doi.org/10.1021/je500770m>
20. Portnov A, Smith A, Mienert J, et al. Offshore permafrost decay and massive seabed methane escape in water depths >20 m at the South Kara Sea Shelf. *Geophys Res Lett*. 2013;40:3962-3967. <https://doi.org/10.1002/grl.50735>
21. Shakhova N, Semiletov I, Leifer I, Salyuk A, Rekant P, Kosmach D. Geochemical and geophysical evidence of methane release over the East Siberian Arctic Shelf. *J Geophys Res Oceans*. 2010;115(C8). <https://doi.org/10.1029/2009JC005602>
22. Shakhova N, Semiletov I, Chuvilin E. Understanding the permafrost-hydrate system and associated methane releases in the East Siberian Arctic Shelf. *Geosciences*. 2019;9(6):251. <https://doi.org/10.3390/geosciences9060251>
23. Shakhova N, Semiletov I, Gustafsson O, et al. Current rates and mechanisms of subsea permafrost degradation in the East Siberian Arctic Shelf. *Nature Communications*. 2017;8:15872. <https://doi.org/10.1038/ncomms15872>
24. Chuvilin E, Ekimova V, Bukhanov B, Grebenkin S, Shakhova N, Semiletov I. Role of salt migration in destabilization of intra permafrost hydrates in the Arctic Shelf: Experimental modeling. *Geosciences*. 2019;9(4):188. <https://doi.org/10.3390/geosciences9040188>
25. Buldovicz SN, Khilimoniyuk VZ, Bychkov AY, et al. Cryovolcanism on the earth: Origin of a spectacular crater in the Yamal Peninsula (Russia). *Sci Rep*. 2018;8:2045-2322. <https://doi.org/10.1038/s41598-018-31858-9>
26. Kizyakov A, Zimin N, Sonyushkin A, Dvornikov Y, Khomutov A, Leibman M. Comparison of gas emission crater geomorphodynamics on Yamal and Gydan peninsulas (Russia), based on repeat very-high-resolution stereopairs. *Remote Sens*. 2017;9(10):1023. <https://doi.org/10.3390/rs9101023>
27. Overduin P, Schneider von Deimling T., Miesner F, et al. Submarine permafrost map in the Arctic modelled using 1d transient heat flux (SuPerMAP). *J Geophys Res Oceans*. 2019;124(6):3490-3507. <https://doi.org/10.1029/2018JC014675>
28. Biskaborn BK, Smith SL, Noetzi J, et al. Permafrost is warming at a global scale. *Nature Commun*. 2019;10:264. <https://doi.org/10.1038/s41467-018-08240-4>
29. NRCAN. Government of Canada GEOSCAN Database. <https://geoscan.nrcan.gc.ca/geoscan-index.html>; 2020.
30. Vigdorichik ME. *Submarine Permafrost on the Alaskan Continental Shelf*. Boulder CO USA: Westview Press; 1980.
31. Vigdorichik ME. *Arctic Pleistocene History and the Development of Submarine Permafrost*. Boulder CO USA: Westview Press; 1980.
32. Serov P, Portnov A, Mienert J, Semenov P, Ilatovskaya P. Methane release from pingo-like features across the South Kara Sea shelf, an area of thawing offshore permafrost. *J Geophys Res Earth Surface*. 2015;120(8):1515-1529. <https://doi.org/10.1002/2015JF003467>
33. Rekant P, Bauch HA, Schwenk T, et al. Evolution of subsea permafrost landscapes in Arctic Siberia since the late Pleistocene: A synoptic insight from acoustic data of the Laptev Sea. *arktos*. 2015;1(1): 11. <https://doi.org/10.1007/s41063-015-0011-1>
34. Portnov A, Mienert J, Winsborrow M, et al. Shallow carbon storage in ancient buried thermokarst in the South Kara Sea. *Sci Rep*. 2018; 8:2045-2322. <https://doi.org/10.1038/s41598-018-32826-z>
35. Yakushev V, Semenov A, Bogoyavlensky V, Medvedev V, Bogoyavlensky I. Experimental modeling of methane release from intrapermafrost relic gas hydrates when sediment temperature change. *Cold Reg Sci Technol*. 2018;149:46-50. <https://doi.org/10.1016/j.coldregions.2018.02.007>
36. Dugan HA, Arcone SA, Obryk MK, Doran PT. High-resolution ground-penetrating radar profiles of perennial lake ice in the McMurdo Dry Valleys, Antarctica: Horizon attributes, unconformities, and subbottom penetration. *Geophysics*. 2016;81(1):WA13-WA20. <https://doi.org/10.1190/geo2015-0159.1>
37. Solomon SM, Taylor AE, Stevens CW. Nearshore ground temperatures, seasonal ice bonding, and permafrost formation within the bottom-fast ice zone, Mackenzie Delta, NWT. In: Proceedings of the Ninth International Conference on Permafrost Kane DL, Hinkel KM, eds., Vol. 2; 2008; Fairbanks, Alaska:1675-1680.
38. Osterkamp TE. Sub-sea permafrost. In: Steele JH, Thorpe SA, Turekian KK, eds. *Encyclopedia of Ocean Sciences*, Vol. 5. New York, London: Academic Press; 2001:2902-2912.
39. Spirina E, Durdenko E, Demidov N, Abramov A, Romanovsky V, Rivkina E. Halophilic-psychrotrophic bacteria of an Alaskan cryopeg—a model for astrobiology. *Paleontol J*. 2017;51(13):1440-1452. <https://doi.org/10.1134/S0031030117120036>
40. French HM, Millar SWS. Permafrost at the time of the Last Glacial Maximum (LGM) in North America. *Boreas*. 2014;43:667-677. <https://doi.org/10.1111/bor.12036>
41. Ward MK, Pollard WH. A hydrohalite spring deposit in the Canadian High Arctic: A potential Mars analogue. *Earth Planetary Sci Lett*. 2018;504:126-138. <https://doi.org/10.1016/j.epsl.2018.10.001>
42. Blasco S, Jenner K, Davies E, et al. Origin and evolution of subsea ice-bearing permafrost on the Canadian Beaufort Shelf: Implication from a 500 m deep borehole. In: Proceedings of Tenth International Conference on Permafrost, Extended Abstracts, Vol. 4. The Northern Publisher (Severnoye Izdatelstvo), Salekhard, Yamal-Nenets Autonomous District; 2012; Russia:56. <https://doi.org/10.1002/2016GC006582>
43. Brothers LL, Herman BM, Hart PE, Ruppel CD. Subsea ice-bearing permafrost on the U.S. Beaufort margin: 1. minimum seaward extent defined from multichannel seismic reflection data. *Geochem Geophys Geosyst*. 2016;17(11):4354-4365. <https://doi.org/10.1002/2016GC006584>
44. Ruppel CD, Herman BM, Brothers LL, Hart PE. Subsea ice-bearing permafrost on the U.S. Beaufort margin: 2. borehole constraints. *Geochem Geophys Geosyst*. 2016;17:4333-4353. <https://doi.org/10.1002/2016GC006582>
45. Brothers LL, Hart PE, Ruppel CD. Minimum distribution of subsea ice-bearing permafrost on the us beaufort sea continental shelf. *Geophys Res Lett*. 2012;39. <https://doi.org/10.1029/2012GL052222>
46. Hu K, Issler DR, Chen Z, Brent TA. Permafrost investigation by well logs, and seismic velocity and repeated shallow temperature surveys, Beaufort-Mackenzie Basin. *Geologic Surv Canada Open File*. 2013; 6956:33. <https://doi.org/10.4095/293120>
47. Rekant P, Vasiliev A. Distribution of subsea permafrost at the Kara Sea Shelf. *Cryosph Earth*. 2011;XV:69-72.
48. Vasiliev AA, Rekant PV, Oblogov GE, Korostelev YV. New GIS-oriented map of submarine permafrost of the Kara Sea. *Reports of the Extended Session of the Scientific Council on Earth Cryology of the Russian Academy of Sciences: Current Problems of Geocryology*, Vol. 1. Moscow: KDU University Press; 2018:291-295. (in Russian).
49. Overduin PP, Haberland C, Ryberg T, et al. Submarine permafrost depth from ambient seismic noise. *Geophys Res Lett*. 2015;42(18): 7581-7588. <https://doi.org/10.1002/2015GL065409>
50. Angelopoulos M, Westermann S, Overduin P, et al. Heat and salt flow in subsea permafrost modeled with CryoGRID2. *J Geophys Res Earth Surface*. 2019;124(4):920-937. <https://doi.org/10.1029/2018JF004823>
51. Overduin PP, Wetterich S, Günther F., et al. Coastal dynamics and submarine permafrost in shallow water of the central Laptev Sea,

- East Siberia. *Cryosphere*. 2016;10(4):1449-1462. <https://doi.org/10.5194/tc-10-1449-2016>
52. Overduin PP, Westermann S, Yoshikawa K, Haberlau TS, Romanovsky V, Wetterich S. Geoelectric observations of the degradation of nearshore submarine permafrost at Barrow (Alaskan Beaufort Sea). *J Geophys Res Earth Surface*. 2012;117(F2). <https://doi.org/10.1029/2011JF002088>
  53. Swarzenski PW, Johnson CD, Lorenson TD, et al. Seasonal electrical resistivity surveys of a coastal bluff, Barter Island, North Slope Alaska. *J Environ Eng Geophys*. 2016;21(1):37-42. <https://doi.org/10.2113/JEEG21.1.37>
  54. Kasprzak M, Strzelecki MC, Traczyk A, Kondracka M, Lim M, Migala K. On the potential for a bottom active layer below coastal permafrost: The impact of seawater on permafrost degradation imaged by electrical resistivity tomography (Hornsund, SW Spitsbergen). *Geomorphology*. 2017;293:347-359. <https://doi.org/10.1016/j.geomorph.2016.06.013>
  55. You Y, Yu Q, Pan X, Wang X, Guo L. Geophysical imaging of permafrost and talik configuration beneath a thermokarst lake. *Permafrost Periglac Process*. 2017;28(2):470-476. <https://doi.org/10.1002/ppp.1938>
  56. Stevens CW, Moorman BJ, Solomon SM, Hugenholtz CH. Mapping subsurface conditions within the near-shore zone of an arctic delta using ground penetrating radar. *Cold Reg Sci Technol*. 2009;56(1):30-38. <https://doi.org/10.1016/j.coldregions.2008.09.005>
  57. Creighton AL, Parsekian AD, Angelopoulos M, et al. Transient electromagnetic surveys for the determination of talik depth and geometry beneath thermokarst lakes. *J Geophys Res Solid Earth*. 2018;123(11):9310-9323. <https://doi.org/10.1029/2018JB016121>
  58. Koshurnikov AV, Tumskey VE, Shakhova NE, et al. The first ever application of electromagnetic sounding for mapping the submarine permafrost table on the Laptev Sea Shelf. *Doklady Earth Sci*. 2016; 469:860-863.
  59. Sherman D, Kannberg P, Constable S. Surface towed electromagnetic system for mapping of subsea arctic permafrost. *Earth Planet Sci Lett*. 2017;460:97-104. <https://doi.org/10.1016/j.epsl.2016.12.002>
  60. Sherman D, Constable SC. Permafrost extent on the Alaskan Beaufort Shelf from surface-towed controlled-source electromagnetic surveys. *J Geophys Res Solid Earth*. 2018;123:7253-7265. <https://doi.org/10.1029/2018JB015859>
  61. Antonova S, Duguay C, Käab A, et al. Monitoring bedfast ice and ice phenology in lakes of the Lena river delta using TerraSAR-X backscatter and coherence time series. *Remote Sens*. 2016;8(11):903. <https://doi.org/10.3390/rs8110903>
  62. Dammann DO, Eriksson LEB, Mahoney AR, Eicken H, Meyer FJ. Mapping pan-Arctic landfast sea ice stability using Sentinel-1 interferometry. *Cryosphere*. 2019;13(2):557-577. <https://doi.org/10.5194/tc-13-557-2019>
  63. Yurganov L, Muller-Karger F, Leifer I. Methane increase over the Barents and Kara Seas after the autumn pycnocline breakdown: Satellite observations. *Adv Polar Sci*. 2019;30(4):382-390.
  64. Batchelor CL, Margold M, Krapp M, et al. The configuration of Northern Hemisphere ice sheets through the Quaternary. *Nature Commun*. 2019;10:1-10. <https://doi.org/10.1038/s41467-019-11601-2>
  65. Gasson EGW, DeConto RM, Pollard D, Clark CD. Numerical simulations of a kilometre-thick Arctic ice shelf consistent with ice grounding observations. *Nature Commun*. 2018;9:1510. <https://doi.org/10.1038/s41467-018-03707-w>
  66. Jakobsson M, Nilsson J, Anderson L, et al. Evidence for an ice shelf covering the Central Arctic Ocean during the penultimate glaciation. *Nature Commun*. 2016;7:10365. <https://doi.org/10.1038/ncomms10365>
  67. Niessen F, Hong JK, Hegewald A, et al. Repeated Pleistocene glaciation of the East Siberian continental margin. *Nature Geosci*. 2013;6: 842-846. <https://doi.org/10.1038/ngeo1904>
  68. Astakhov VI. Pleistocene glaciations of northern Russia - a modern view. *Boreas*. 2013;42:1-24. <https://doi.org/10.1111/j.1502-3885.2012.00269.x>
  69. Batchelor CL, Dowdeswell JA, Pietras JT. Seismic stratigraphy, sedimentary architecture and palaeo-glaciology of the Mackenzie Trough: evidence for two Quaternary ice advances and limited fan development on the Western Canadian Beaufort Sea margin. *Quatern Sci Rev*. 2013;65:73-87. <https://doi.org/10.1016/j.quascirev.2013.01.021>
  70. Batchelor CL, Dowdeswell JA, Pietras JT. Evidence for multiple Quaternary ice advances and fan development from the Amundsen Gulf cross-shelf trough and slope, Canadian Beaufort Sea margin. *Marine Petrol Geology*. 2014;52:125-143. <https://doi.org/10.1016/j.marpetgeo.2013.11.005>
  71. Farquharson L, Mann D, Rittenour T, Groves P, Grosse G, Jones B. Alaskan marine transgressions record out-of-phase Arctic Ocean glaciation during the last interglacial. *Geology*. 2018;46:783-786. <https://doi.org/10.1130/G40345.1>
  72. Klemann V, Heim B, Bauch HA, Wetterich S, Opel T. Sea-level evolution of the Laptev Sea and the East Siberian Sea since the Last Glacial Maximum. *arktos*. 2015;1(1):1. <https://doi.org/10.1007/s41063-015-0004-x>
  73. Obu J, Westermann S, Bartsch A, et al. Northern hemisphere permafrost map based on TTOP modelling for 2000-2016 at 1 m2 scale. *Earth-Sci Rev*. 2019;193:299-316. <https://doi.org/10.1016/j.earscirev.2019.04.023>
  74. Overduin PP, Schneider von Deimling T, Miesner F, et al. Submarine Permafrost Map (SuPerMAP), modeled with CryoGrid 2, Circum-Arctic. <https://doi.pangaea.de/10.1594/PANGAEA.910540>. Supplement to: Overduin, Pier Paul; Schneider von Deimling, Thomas; Miesner, Frederieke; Grigoriev, Mikhail N; Ruppel, Carolyn D; Vasiliev, Alexander A; Lantuit, Hugues; Juhls, Bennet; Westermann, Sebastian (2019): Submarine Permafrost Map in the Arctic Modeled Using 1-D Transient Heat Flux (SuPerMAP). *Journal of Geophysical Research: Oceans*, 124(6), 3490-3507, <https://doi.org/10.1029/2018JC014675>; 2020.
  75. Obu J, Westermann S, Käab A, Bartsch A. Ground Temperature Map, 2000-2016, Northern Hemisphere Permafrost. <https://doi.org/10.1594/PANGAEA.888600>; 2018.
  76. Grigoriev MN. Kriomorphogenez i litodinamika pribrezhno-shelfovoi zony morei vostochnoi sibirii (cryomorphogenesis and lithodynamics of the East Siberian near-shore shelf zone). *Habilitation thesis*; 2008.
  77. Grigoriev MN, Kunitsky VV, Chzhan RV, Shepelev VV. On the variation in geocryological, landscape and hydrological conditions in the Arctic zone of East Siberia in connection with climate warming. *Geograph Natural Resources*. 2009;30(2):101-106. <https://doi.org/10.1016/j.gnr.2009.06.002>
  78. Jones BM, Farquharson LM, Baughman CA, et al. A decade of remotely sensed observations highlight complex processes linked to coastal permafrost bluff erosion in the Arctic. *Environ Res Lett*. 2018; 13(11):115001. <https://doi.org/10.1016/10.1088/1748-9326/aae471>
  79. Irrgang AM, Lantuit H, Manson GK, Günther F, Grosse G, Overduin PP. Variability in rates of coastal change along the Yukon coast, 1951 to 2015. *J Geophys Res Earth Surface*. 2018;123(4):779-800. <https://doi.org/10.1002/2017JF004326>
  80. Schirrmeyer L, Grigoriev M, Strauss J, et al. Sediment characteristics of a thermokarst lagoon in the northeastern Siberian Arctic (Ivashkina Lagoon, Bykovsky Peninsula). *arktos*. 2018;4:13. <https://doi.org/10.1007/s41063-018-0049-8>

81. Dugan HA, Lamoureux SF. The chemical development of a hypersaline coastal basin in the High Arctic. *Limnol Oceanograph*. 2011;56(2):495-507. <https://doi.org/10.4319/lo.2011.56.2.0495>
82. Harris CM, McClelland JW, Connelly TL, Crump BC, Dunton KH. Salinity and temperature regimes in Eastern Alaskan Beaufort Sea lagoons in relation to source water contributions. *Estuaries Coasts*. 2017;40(1):50-62. <https://doi.org/10.1007/s12237-016-0123-z>
83. Lecher AL, Kessler J, Sparrow K, et al. Methane transport through submarine groundwater discharge to the North Pacific and Arctic Ocean at two Alaskan sites. *Limnol Oceanograph*. 2016;61(S1):S344-S355. <https://doi.org/10.1002/lno.10118>
84. Charkin AN, Rutgers van der Loeff M., Shakhova NE, et al. Discovery and characterization of submarine groundwater discharge in the Siberian Arctic seas: a case study in the Buor-Khaya Gulf, Laptev Sea. *Cryosphere*. 2017;11(5):2305-2327. <https://doi.org/10.5194/tc-11-2305-2017>
85. Gwiazda R, Paull C, Dallimore S, et al. Freshwater seepage into sediments of the shelf, shelf edge, and continental slope of the Canadian Beaufort Sea. *Geochem Geophys Geosyst*. 2018;19(9):3039-3055. <https://doi.org/10.1029/2018GC007623>
86. JuhlsBennet, Stedmon Colin A., Morgenstern Anne, Meyer Hanno, Hölemann Jens, Heim Birgit, Povazhnyi Vasily, Overduin Pier P. Identifying Drivers of Seasonality in Lena River Biogeochemistry and Dissolved Organic Matter Fluxes. *Frontiers in Environmental Science*. 2020;8. <http://dx.doi.org/10.3389/fenvs.2020.00053>
87. Fedorova I, Chetverova A, Bolshiyarov D, et al. Lena Delta hydrology and geochemistry: long-term hydrological data and recent field observations. *Biogeosciences*. 2015;12(2):345-363. <https://doi.org/10.5194/bg-12-345-2015>
88. Semenov P, Portnov A, Krylov A, Egorov A, Vanshtein B. Geochemical evidence for seabed fluid flow linked to the subsea permafrost outer border in the South Kara Sea. *Geochemistry*. 2019:125509. <https://doi.org/10.1016/j.chemer.2019.04.005>
89. Romanovskii N, Hubberten H-W, Gavrilov A, Eliseeva A, Tipenko G. Offshore permafrost and gas hydrate stability zone on the shelf of East Siberian Seas. *Geo-Marine Lett*. 2005;25(2-3):167-182. <https://doi.org/10.1007/s00367-004-0198-6>
90. Mitzscherling J, Winkel M, Winterfeld M, et al. The development of permafrost bacterial communities under submarine conditions. *J Geophys Res Biogeosci*. 2017;122:1689-1704. <https://doi.org/10.1002/2017JG003859>
91. Winkel M, Mitzscherling J, Overduin PP, et al. Anaerobic methanotrophic communities thrive in deep submarine permafrost. *Sci Rep*. 2018;8:1291. <https://doi.org/10.1038/s41598-018-19505-9>
92. Winkel M, Sepulveda-Jauregui A, Martinez-Cruz K, et al. First evidence for cold-adapted anaerobic oxidation of methane in deep sediments of thermokarst lakes. *Environ Res Commun*. 2019;1(2):021002. <https://doi.org/10.1088/2515-7620/ab1042>
93. Sparrow KJ, Kessler JD, Southon JR, et al. Limited contribution of ancient methane to surface waters of the U.S. Beaufort Sea Shelf. *Sci Adv*. 2018;4. <https://doi.org/10.1126/sciadv.aao4842>
94. Damm E, Bauch D, Krumpfen T, et al. The Transpolar Drift conveys methane from the Siberian Shelf to the Central Arctic Ocean. *Sci Rep*. 2018;8:1-10. <https://doi.org/10.1038/s41598-018-22801-z>
95. Shakhova N, Semiletov I, Leifer I, et al. Ebullition and storm-induced methane release from the East Siberian Arctic Shelf. *Nature Geosci*. 2014;7:64-70. <https://doi.org/10.1002/2015JF003467>
96. Frederick J, Buffett B. Taliks in relict submarine permafrost and methane hydrate deposits: Pathways for gas escape under present and future conditions. *J Geophys Res Earth Surface*. 2014;119(2):106-122. <https://doi.org/10.1002/2013JF002987>
97. Grosse G, Romanovsky V, Jorgenson T, Walter Anthony K, Brown J, Overduin PP. Vulnerability and feedbacks of permafrost to climate change. *EOS Trans*. 2011;92(9):73-74. <https://doi.org/10.1029/2011EO090001>
98. Fisher RE, Srisankharajah S, Lowry D, et al. Arctic methane sources: Isotopic evidence for atmospheric inputs. *Geophys Res Lett*. 2011;38. <https://doi.org/10.1029/2011GL049319>
99. Thornton BF, Geibel MC, Crill PM, Humborg C, Mörth C-M. Methane fluxes from the sea to the atmosphere across the Siberian Shelf seas. *Geophys Res Lett*. 2016;43:5869-5877. <https://doi.org/10.1002/2016GL068977>
100. Mestdagh T, Poort J, Batist MD. The sensitivity of gas hydrate reservoirs to climate change: Perspectives from a new combined model for permafrost-related and marine settings. *Earth Sci Rev*. 2017;169:104-131. <https://doi.org/10.1016/j.earscirev.2017.04.013>
101. Dmitrenko IA, Kirillov SA, Tremblay LB, et al. Recent changes in shelf hydrography in the Siberian Arctic: Potential for subsea permafrost instability. *J Geophys Res Oceans*. 2011;116(C10). <https://doi.org/10.1029/2011JC007218>
102. Golubeva E, Platov G, Malakhova V, Kraineva M, Iakshina D. Modelling the long-term and inter-annual variability in the Laptev Sea hydrography and subsea permafrost state. *Polarforschung*. 2018;87:195-210. <https://doi.org/10.2312/polarforschung.87.2.195>
103. Kunitsky VV. *Kriolitologiya/Nizovaya Leny (Cryolithology of the Lower Lena)*. Yakutsk: Melnikov Permafrost Institute, Russian Academy of Sciences, Siberian Branch; 1989. (in Russian).
104. Overduin PP, Liebner S, Knoblauch C, et al. Methane oxidation following submarine permafrost degradation: Measurements from a Central Laptev Sea shelf borehole. *J Geophys Res Biogeosci*. 2015;120(5):965-978. <https://doi.org/10.1002/2014JG002862>
105. Overduin PP, Rachold V, Grigoriev MN. The state of subsea permafrost in the Western Laptev nearshore zone. In: Ninth International Conference on Permafrost Kane DL, Hinkel, KM ed., Fairbanks, Alaska; 2008:1345-1350.
106. Harrison W, Osterkamp TE. Heat and mass transport processes in subsea permafrost 1. An analysis of molecular diffusion and its consequences. *J Geophys Res Oceans*. 1978;83(C9):4707-4712.
107. Harding-Lawson Associates (HL). USGS technical investigation beaufort sea-1979. Technical Report, United States Geological Survey; 1979. (2 vols.)
108. Taylor AE, Dallimore SR, Hill PR, Issler DR, Blasco S, Wright F. Numerical model of the geothermal regime on the Beaufort Shelf, arctic Canada since the Last Interglacial. *J Geophys Res Earth Surf*. 2013;118:2365-2379. <https://doi.org/10.1002/2013JF002859>
109. Roy-Leveille P, Burn CR. Near-shore talik development beneath shallow water in expanding thermokarst lakes, Old Crow Flats, Yukon. *J Geophys Res Earth Surface*. 2017;122(5):1070-1089. <https://doi.org/10.1002/2016JF004022>
110. Malakhova VV, Eliseev AV. The role of heat transfer time scale in the evolution of the subsea permafrost and associated methane hydrates stability zone during glacial cycles. *Global Planet Change*. 2017;157:18-25. <https://doi.org/10.1016/j.jglplacha.2017.08.007>
111. Bogorodskii PV, Pnyushkov AV, Kustov VY. Seasonal freezing of a submarine ground layer at the Laptev Sea Shelf. In: Velarde MG, Tarakanov RY, Marchenko AV, eds. *The Ocean in Motion: Circulation, Waves, Polar Oceanography*. Cham: Springer International Publishing; 2018:611-625. [https://doi.org/10.1007/978-3-319-71934-4\\_39](https://doi.org/10.1007/978-3-319-71934-4_39)
112. Romanovskii NN, Hubberten H-W. Results of permafrost modelling of the lowlands and shelf of the Laptev Sea region, Russia. *Permafrost Periglacial Process*. 2001;12(2):191-202. <https://doi.org/10.1002/ppp.387>
113. Malakhova VV. On the thermal influence of thermokarst lakes on the subsea permafrost evolution. In: 22nd International Symposium on Atmospheric and ocean Optics: Atmospheric Physics, Vol. 10035 International Society for Optics and Photonics; 2016; Tomsk, Russian Federation:100355U. <https://doi.org/10.1117/12.2248714>

114. Nicolsky D. J., Romanovsky V. E., Romanovskii N. N., Kholodov A. L., Shakhova N. E., Semiletov I. P. Modeling sub-sea permafrost in the East Siberian Arctic Shelf: The Laptev Sea region. *Journal of Geophysical Research: Earth Surface*. 2012;117(F3):n/a–n/a. <http://dx.doi.org/10.1029/2012jf002358>
115. Nicolsky D, Shakhova N. Modeling sub-sea permafrost in the East Siberian Arctic Shelf: The Dmitry Laptev Strait. *Environ Res Lett*. 2010;5:015006. <https://doi.org/10.1088/1748-9326/5/1/015006>
116. Razumov SO, Spektor VB, Grigoriev MN. A model of the late Cenozoic cryolithozone evolution for the Western Laptev Sea Shelf. *Okeanologiya*. 2014;54(5):679–693.
117. Janout MA, Hölemann J, Timokhov L, Gutjahr O, Heinemann G. Circulation in the northwest Laptev Sea in the Eastern Arctic Ocean: Crossroads between Siberian river water, Atlantic water and polynya-formed dense water. *J Geophys Res Oceans*. 2017;122(8):6630–6647. <https://doi.org/10.1002/2017JC013159>
118. Portnov A, Mienert J, Serov P. Modeling the evolution of climate-sensitive Arctic subsea permafrost in regions of extensive gas expulsion at the West Yamal Shelf. *J Geophys Res Biogeosci*. 2014;119:2082–2094. <https://doi.org/10.1002/2014JG002685>

**How to cite this article:** Angelopoulos M, Overduin PP, Miesner F, Grigoriev MN, Vasiliev AA. Recent advances in the study of Arctic submarine permafrost. *Permafrost and Periglac Process*. 2020;31:442–453. <https://doi.org/10.1002/ppp.2061>